NUKLEONIKA 2013;58(1):189–194

ORIGINAL PAPER

Photoluminescence and positron annihilation lifetime studies on pellets of ZnO nanocrystals

Andrzej Karbowski,
Kamil Fedus,
Jaromir Patyk,
Łukasz Bujak,
Krzysztof Służewski,
Grzegorz Karwasz

Abstract. We explore the interrelationships between the X-ray diffraction patterns, the photoluminescence spectra and the positron lifetimes obtained from circular pellets composed of commercial ZnO nanoparticles. The experimental results are studied as a function of thermal treatment at different temperatures. X-ray diffractograms reveal the temperature-independent wurtzite phase structure of nanocrystals and show huge enlargement of ZnO grains after annealing at temperatures higher than 700°C. Photoluminescence measurements exhibit two emission bands: a near band edge emission in UV (~378 nm) and a defect-related broad visible peak with a maximum in the green region (~502 nm). The significant enhancement of the green emission at the expense of UV luminescence is observed after sample sintering at 800 and 1000°C. The positron annihilation lifetime spectroscopy (PALS) is applied in order to study the thermally induced evolution of defects. The lifetime components show a step-like dependence on the thermal treatment, but do not follow exactly the variation in crystallographic phases and only vaguely follow differences in photoluminescence. The positron data indicate therefore some additional structural and/or defect changes. The possible origin of green luminescence from ZnO pellets is discussed.

Key words: photoluminescence (PL) • positron annihilation lifetime spectroscopy (PALS) • X-ray diffraction (XRD) • ZnO nanocrystals

A. Karbowski, K. Fedus✉, J. Patyk, Ł. Bujak,
K. Służewski, G. Karwasz
Nicolaus Copernicus University,
Institute of Physics,
5/7 Grudziądzka Str., 87-100 Toruń, Poland,
Tel.: +48 56 611 3291, Fax: +48 56 622 5397,
E-mail: kamil@fizyka.umk.pl

Received: 14 June 2012
Accepted: 10 October 2012

Introduction

Zinc oxide (ZnO) is a material with great potential for a variety of practical applications due to the unique physical and chemical properties such as wide and direct energy band gap (~3.37 eV), large exciton binding energy (~60 meV), high electron mobility, high thermal conductivity, high radiation damage resistance and biocompatibility. The recent progress in nanoscaling of ZnO structures attracts also attention towards the use of ZnO in nanotechnological applications. Therefore, mechanical, electrical and optical properties of nanostructured ZnO crystals are widely investigated in different conditions by many research groups [5, 6, 14]. However, in spite of the numerous studies, not all mechanisms responsible for physical phenomena in ZnO are fully understood. One of the problems concerns the origin of spontaneous emission which has been broadly investigated by photoluminescence (PL) spectroscopy. Typically, the room temperature spectra of ZnO consist of a UV emission and possibly one or more visible bands (violet [21, 33], blue [24, 31], green [4, 8, 9, 11, 12, 19, 22, 25, 27–29, 32, 34] or yellow-orange-red [20, 23]). The origin of the UV peak is well explained because it is related to the near-band-edge

excitonic transitions. Whereas the visible emissions are assigned to defects and/or impurities. However finding the exact explanations for each peak are complicated because their spectral positions and the intensities strongly depend on the fabrication process [18]. Growth procedures determine concentrations of intrinsic and extrinsic defects as well as the spices of impurities. The created luminescent centres must to be identified as a function of preparation procedure in order to understand and control ZnO properties. Particularly, a number of different hypothesis have been proposed in order to explain the most frequently observed green emission. Propositions include the involvement of Cu impurities [8], Zn vacancies [27, 29, 34], oxygen vacancies [9, 12, 25, 28, 32], oxide antisite defects [19] or surface defects/defects complexes [4, 11]. However, no consensus has been reached and the topic remains controversial. What is worse, there are also huge discrepancies between theoretical models of defects in ZnO. Different studies predict different energy levels for the same type of defect and, consequently, no constructive conclusions can be made (see Ref. [6] and references therein). As pointed out in Ref. [6], the difficulties in identifying the origin of defects bands in ZnO is the fact that the bands are broad and overlapping. In the light of all these problems it is necessary to make as many measurements as possible on different samples using different characterization techniques in various experimental conditions in order to obtain a final reliable picture of phenomenon. The aim of this paper is to add another contribution to studies on green luminescence in ZnO. In particular, we investigated the effect of thermal treatment on spontaneous emission from circular pellets composed of ZnO nanocrystals. The study is supported by two complementary characterization techniques: X-ray diffraction (XRD) and positron annihilation lifetime spectroscopy (PALS). Both methods provide valuable insights into defects, structure and size of nanoparticles. The correlation between results obtained from these different experiments is presented and the possible origin of green luminescence in ZnO is discussed.

Experiments

Commercially available powders composed of ZnO nanoparticles were purchased from Sigma Aldrich with a purity of 99.7% and a specific surface area of 15–25 m^2/g. Pellets of 1 cm diameter and 1 mm thickness were formed under 250 MPa pressure at room temperature. They were subsequently annealed in open air at 8 different temperatures: 150, 200, 400, 500, 600, 700, 800 and 1000°C for 12 h in an electric muffle furnace. Crystallinity and size of nanoparticles were investigated by the standard XRD measurement (theta-2 theta mode) using powder X-ray diffractometer (Siemens D5000). The setup was equipped with a copper X-ray lamp, nickel K_β filter and 8° wide position sensitive detector (PSD) used with an argon (90%)-methane (10%) mixture gas. The room temperature photoluminescence spectra were recorded on a Horiba-Jobin-Ivon SPEX Fluorog 3-22 spectrometer. A xenon lamp was used as excitation light source with excitation wavelength at 325 nm.

Positron annihilation lifetime spectroscopy was used to investigate thermally induced evolution of defects in ZnO nanocrystals. Positron trapping in open-volume defects, such as in vacancies and their agglomerates, causes an increase of the positron lifetime with respect to the defect-free samples. This is due to the locally reduced electron density of the defects. PALS is a powerful method to identify defects since the annihilation characteristics of positrons can be often assigned to particular trapped states. The experiments were carried out using the fast-fast coincidence ORTEC PLS system equipped with plastic scintillators (St. Gobain BC418) and RCA 8850 photomultipliers [16]. The prompt time resolution of the system was 180 ps in full width at half maximum (FWHM). The positron source $^{22}NaCl$ (10 μCi) in a kapton 7 μm thick foil was sandwiched between two identical ZnO pellets. At least 10^6 total counts were accumulated in each measurement. Several runs were performed for each of the two identical samples. The analysis of lifetime spectra was realized with the LT package created by Kansy [15].

Results and discussion

X-ray diffraction

Typical XRD patterns of the ZnO pellets prepared from as-purchased powder and powders annealed at 400, 800 and 1000°C are shown in Fig. 1. The ZnO samples exhibit good crystallinity with no obvious indication for the existence of amorphous domains – all diffraction peaks can be readily indexed as hexagonal wurtzite ZnO crystal structure. No phase transition was observed between as-purchased and annealed at 1000°C powders. In addition, the intensity of the peaks increases and the FWHM decreases with the increasing annealed temperature, which indicates a possible change in the grain size. This aspect was analyzed with Bruker Physic TOPAS software [17].

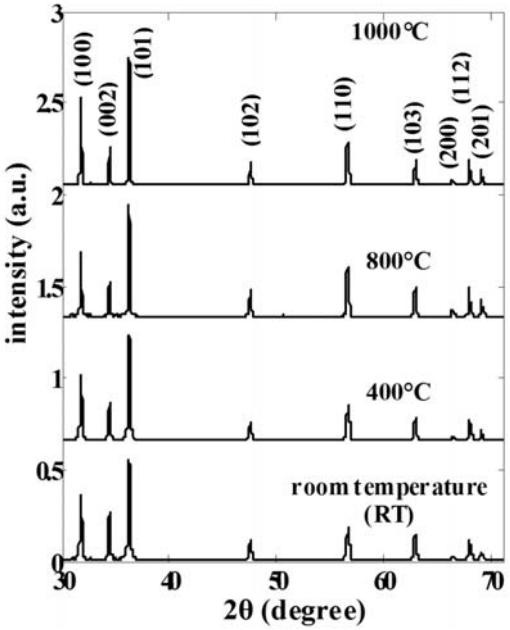

Fig. 1. XRD patterns for the as-purchased and annealed at 400, 800 and 1000°C ZnO nanocrystals.

Table 1. ZnO nanocrystallite size depending on temperature of sintering

No.	Sample	Lorentz diameter (nm)	Volume diameter (nm)
1	powder	94.9 ± 0.6	84.42 ± 0.54
2	400°C	95.3 ± 0.6	84.8 ± 0.6
3	800°C	246.8 ± 4.2	220 ± 4
4	1000°C	293 ± 7	261 ± 6

Whole pattern fitting was performed using ZnO structure data (the hexagonal wurtzite phase) with fundamental parameters (FP) profile shape of diffraction reflexes. This procedure allowed to eliminate impact of $K\alpha_2$ emission line of copper on the registered diffraction data. The average diameters of nanocrystallites were estimated using two algorithms: one Scherrer-like algorithm using a Lorentz shape peak and the second calculated as volume mean weighted using a Lorentz and Gauss convoluted peak shape. The determined sizes are presented in Table 1. Both numerical procedures give results which are in very good agreement. Annealing up to 400°C does not change noticeably the size of ZnO nanoparticles, while sintering at higher temperatures corresponds to a significant increase of nanocrystallites. The particle diameters are enlarged by approximately 180–200 nm after annealing at 1000°C. This can be explained by a thermally-induced agglomeration of grains in the samples [29]. A similar effect has been already observed in Ref. [12] where ZnO pellets have been investigated in the same temperature range.

It has to be highlighted that no quantum confinement effect should be expected for these samples since the sizes are much larger than the exciton Bohr radius in ZnO (approximately 2.34 nm [10]). Hence the quantum effects are expected to have no influence on spontaneous emission spectra presented in the next section.

Photoluminescence

Figure 2a presents the room temperature photoluminescence spectra of ZnO nanocrystals annealed at different temperatures. As typically the spectra exhibit two emission peaks: one in UV with a maximum at 375–380 nm and the second in the visible (green) region peaking at 502–510 nm. Several interesting things can be noticed from the measured data. The luminescence spectrum obtained from the as-purchased powder (RT) consists of approximately equal UV and visible peaks. Whereas the annealing at elevated temperatures to 600–700°C induces continuous quenching of UV emission such that the ratio of heights of the visible-to-UV peaks, shown in Fig. 2b, is increased by a factor of two. Moreover, the shift of the visible peak towards the longer wavelengths is also observed in this range of temperatures. Further increase of sintering temperature up to 800 and 1000°C results in significant enhancement of visible emission and very deep reduction of UV peak. The small shift of the UV emission towards shorter wavelengths is also observed. A plausible explanation of thermally induced quenching of excitonic emission could be the energy band bending due to the chemisorption of oxygen at the ZnO surface as described recently in Ref. [30]. This adsorption can occur in the air in normal conditions and increase with ambient temperature, producing an upward band bending and a surface depletion. A large ZnO absorption coefficient of ~160 000 cm^{-1} at 325 nm corresponds to a penetration depth of ~60 nm. Therefore, upon excitation, most of the electrons and holes are generated near the surface where they are swept to the opposite directions across the depletion region, thus reducing their chances of recombination through excitonic processes. This model is confirmed by many experiments showing that surface passivation by coating ZnO nanostructures with different materials results in suppressing green emission and enhancing UV luminescence (see Ref. [30] and references therein). Furthermore, the authors of Ref. [30] suggest that the oxygen chemisorption is accompanied by the creation of oxygen vacancies (V_O) in the depletion region. This can explain the significant enhancement of green luminescence observed in this work after annealing the samples at temperatures higher than 700°C. Nevertheless, this phenomenon requires further investigation, especially the attention should be paid to the obvious correlation of the latter effects with the thermally-induced grain enlargement reported in the previous section as well as in Ref. [29] for similar samples.

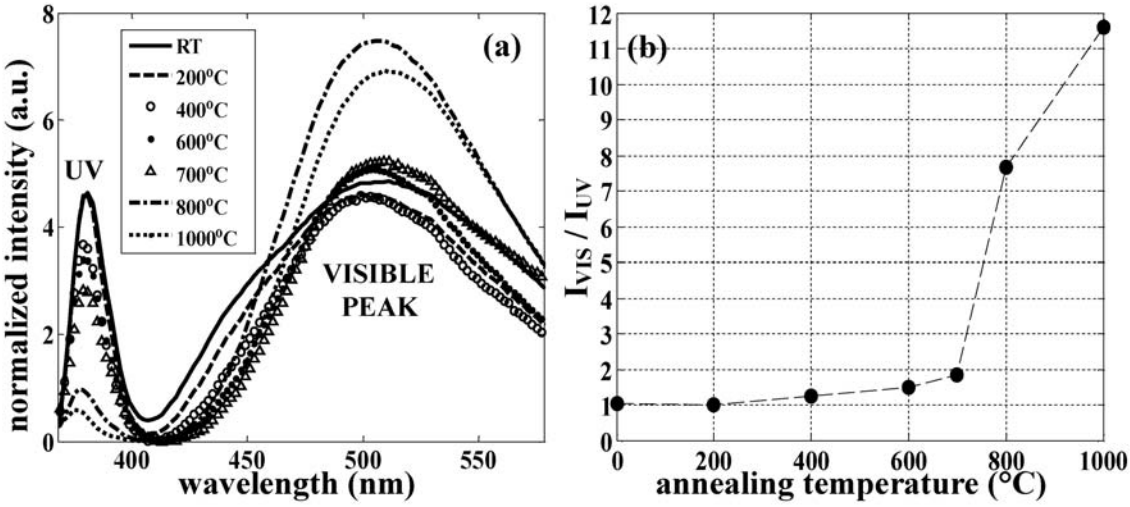

Fig. 2. (a) Photoluminescence spectra of ZnO pellets annealed at different temperatures for an excitation wavelength of 325 nm; (b) the ratio of heights of visible to UV emission peaks (I_{VIS}/I_{UV}) in function of annealing temperature.

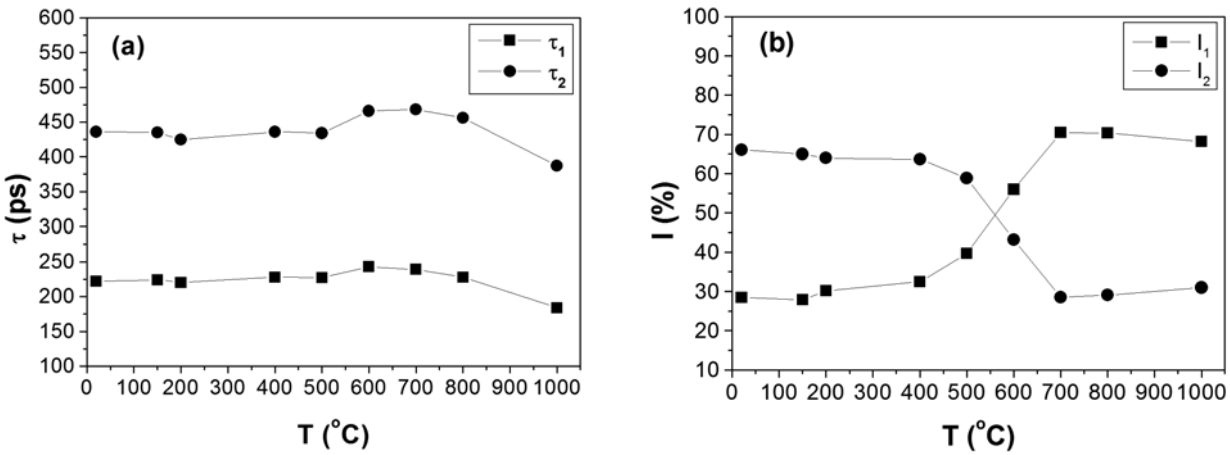

Fig. 3. (a) Positron lifetimes τ_1 and τ_2 and (b) relative intensities I_1 and I_2 as a function of annealing temperatures in ZnO samples.

Positron annihilation lifetime spectroscopy

The LT analysis of measured positron lifetime spectra reveals three components: a short lifetime τ_1 of about 220–230 ps (see Fig. 3a), an intermediate lifetime τ_2 of about 430–440 ps (see Fig. 3a) and very long lifetime τ_3 of about 60 ns (see Fig. 4a) obtained in the sample prepared from as-purchased powder. The existence of three components is in very good agreement with positron lifetime data published on ZnO nanoparticles by other research groups [21, 26, 29].

According to the most popular hypothesis, the shortest lifetime (τ_1) corresponds to positron trapping in zinc vacancies (V_{Zn}) [2, 3, 21, 29, 30] located either in the bulk or/and on the particle surface referred to as grain boundary. This assumptions is based on experimental and theoretical works showing that V_{Zn} together with oxygen vacancy (V_O) are dominant in ZnO because they are characterized by low formation energies [13]. However, only the negatively charged V_{Zn} is visible to the positrons since the positively charged V_O has too low positron binding energy [3, 27]. Additionally, it is expected that the most efficient trapping occurs on the grain boundaries. This is because the average positron diffusion length could be as large as 150–200 nm [1], so it is usually enough to let positrons reach the grain boundaries during thermalization inside nanocrystallites. Moreover, theoretical calculations [7] predict that the formation energy of zinc vacancy is lower at grain boundaries than that in the bulk, hence the surface of ZnO nanoparticles is rich in vacancy defects. This experimental work shows that after sample treatment at 150–700°C, τ_1 keeps relatively constant (230–240 ps, see Fig. 3a). It means that the grain growth does not influence noticeably on positron annihilations centres responsible for this component. But after annealing at 1000°C, τ_1 decreases rapidly to 184 ps. The latter value is close to the positron bulk lifetime reported in hydrothermal grown ZnO [29]. The sudden fall in τ_1 value can be explained by a thermally induced recovery of both, grain boundary and bulk located Zn vacancies. Consequently, most positrons annihilate in the bulk and/or in other kind of defects or imperfection left in the sample. If this interpretation is correct, one could conclude that zinc vacancies (V_{Zn}) are not responsible for a green luminescence. Indeed, the reduction of V_{Zn} concentration cannot explain the observed enhancement of green emission at the very same samples. Nevertheless, the ultimate conclusion cannot be made yet due to a difference in sample penetration depths in PL and PALS methods. The penetration depth for the excitation light (λ = 325 nm) is about 60 nm and PL occurs mainly on the surface [30], while positrons penetrate the whole volume of the sample. Hence the contributions of defects on surface and in bulk of nanocrystals to positron lifetimes should be separated in order to obtain clearer picture. Depth-resolved positron annihilation studies would help in solving this question.

The second lifetime τ_2 does not have such a straightforward interpretation as τ_1. For example, in Ref. [21] this component is assigned to positron trapping in nanovoids at the intersection of grain boundaries, while in Ref. [29] τ_2 is related to the 6-$V_{Zn}V_O$ vacancy cluster located at the grain surface. Nevertheless, it can be generally assumed that this component is somehow associated with positron annihilation in the grain interface region. Therefore, the reason of the reduction in I_2 at temperatures higher than 400°C shown in Fig. 3b can be attributed to the smaller fraction of positrons annihilating at the surface and interface region as a result of grain enlargement. The observed increase of τ_2 from 430 ps to about 470 ps after annealing at 150–700°C should be assigned to the formation of some vacancy clusters in this region, while a sudden decrease of τ_2 to 390 ps at 1000°C can be related to decompositions of this complex defects (see Fig. 3a).

There is common agreement that the longest lifetime component τ_3 should be assigned to the annihilation of *ortho*-positronium formed in large voids in the intercrystalline regions [21, 29]. Figure 4 shows that when the annealing temperature increases from 150 to 1000°C, τ_3 decreases very fast from 60 to 2 ns and the relative intensity I_3 changes from 5.5 to 0.8%. This drop is particularly rapid between 400 to 500°C. These results are in very good agreement with the data reported in Refs. [21, 29] and are to be attributed to the sintering process. Namely, the gradual decrease of τ_3 suggests the reduction of intercrystalline free volume concentration due to the thermally induced agglomeration of grains in the samples.

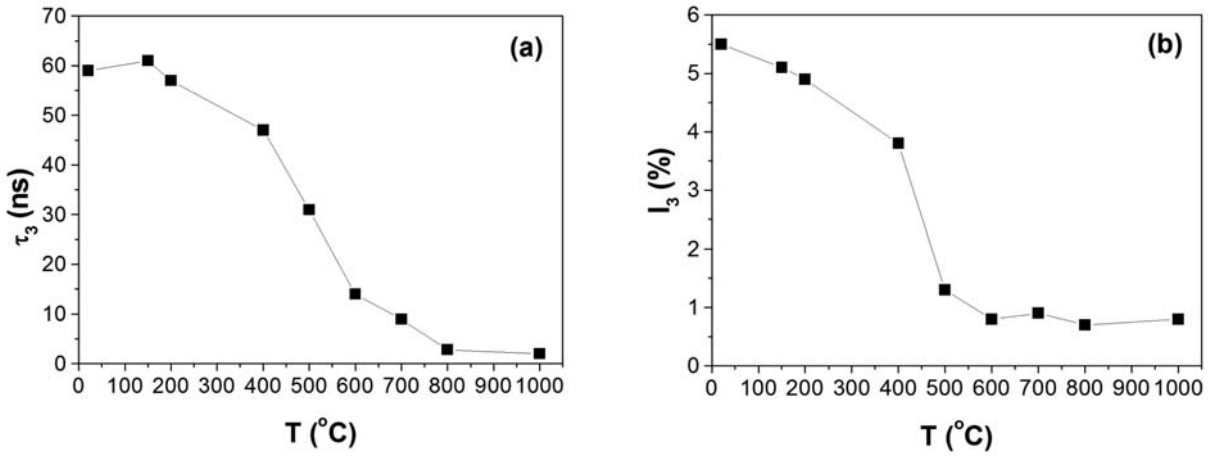

Fig. 4. (a) Long lifetime component τ_3 and (b) relative intensities I_3 as a function of annealing temperatures in ZnO samples.

Conclusions

The disc-shape pellets composed of ZnO nanoparticles were prepared and annealed at different temperatures in the range of 150–1000°C, and then subsequently studied by X-ray diffraction, photoluminescence and positron lifetime annihilation methods. All techniques reveal significant changes in properties of nanoparticles with annealing temperatures. In particular the large enhancement of green luminescence at the expense of near-band-edge UV emission is observed after thermal treatment at temperatures higher than 700°C. Moreover, PALS measurements show no correlation between zinc vacancies (V_{Zn}) and defect-induced green emission – the drop in the intensity of the intermediate component (about 450 ps) occurs rapidly between 500 and 700°C, distinctly below the temperature (800°C) where the green photoluminescence starts to dominate. More studies should be carried out in order to identify the kind of structural and/or defect variations in this (500 to 800°C) range of temperatures and to exclude ultimately V_{Zn} as green luminescence centres. Since it is expected that the green emission originates mainly from the surface of ZnO nanocrystals, thus PL and PALS should be measured and compared in samples treated thermally in different atmospheric conditions. Particularly, oxygen-rich and oxygen-poor environments should be considered in order to investigate the influence of oxidation on PL and PALS measurements. These studies are in progress.

Acknowledgment. One of the authors (Ł. Bujak) would like to acknowledge the support by the WELCOME programme "Hybrid nanostructures as a stepping-stone towards efficient artificial photosynthesis" from the Foundation for Polish Science. Fluorescence measurements were carried out at the facilities of National Laboratory FAMO in the Institite of Physics, NCU in Toruń. The ORTEC PLS system has been purchased within the NLTK laboratories (grant no. POIG 02.02.00-00-003/08) at NCU in Toruń.

References

1. Borseth TM, Tuomisto F, Christensen JS *et al*. (2006) Deactivation of Li by vacancy clusters in ion-implanted and flash-annealed ZnO. Phys Rev B 74:161202(R)
2. Brauer G, Kuriplach J, Cizek J *et al*. (2007) Positron lifetimes in ZnO single crystals. Vacuum 81:1314–1317
3. Chen ZQ, Yamamoto S, Maekawa M, Kawasuso A, Yuan XL, Sekiguchi T (2003) Postgrowth annealing of defects in ZnO studied by positron annihilation, X-ray diffraction, Rutherford backscattering, cathodoluminescence, and Hall measurements. J Appl Phys 94:4807–4812
4. Djurisic AB, Choy WCH, Roy VAL *et al*. (2004) Photoluminescence and electron paramagnetic resonance of ZnO tetrapod structures. Adv Funct Mater 14;9:856–864
5. Djurisic AB, Leung YH (2006) Optical properties of ZnO nanostructures. Small 2;8/9:944–961
6. Djurisic AB, Ng AMC, Chen XY (2010) ZnO nanostructures for optoelectronics: Material properties and device applications. Prog Quant Electron 34:191–259
7. Domingos HS, Carlsson JM, Bristowe PD, Hellsing B (2004) The formation of defect complexes in a ZnO grain boundary. Interface Sci 12:227–234
8. Garces NY, Wang L, Bai L, Giles NC, Halliburton LE, Cantwell G (2002) Green luminescent ZnO:Cu^{2+} nanoparticles for their applications in white-light generation from UV LEDs. Appl Phys Lett 81;4:622–624
9. Gong Y, Andelman T, Neumark GF, O'Brien S, Kuskovsky IL (2007) Origin of defect-related green emission from ZnO nanoparticles: effect of surface modification. Nanoscale Res Lett 2:297–302
10. Gu Y, Kuskovsky I, Yin M, O'Brien S, Neumark GF (2004) Quantum confinement in ZnO nanorods. Appl Phys Lett 85:3833–3835
11. Guo L, Yang S, Yang C, Yu P, Wang J, Ge W, Wong GKL (2000) Highly monodisperse polymer-capped ZnO nanoparticles: Preparation and optical properties. Appl Phys Lett 76:2901–2903
12. Irimpan L, Nampoori VPN, Radhakrishnan P, Deepthy A, Krishnan B (2007) Size dependent fluorescence spectroscopy of nanocolloids of ZnO. J Appl Phys 102:063524
13. Janotti A, Van de Walle CG (2007) Native point defects in ZnO. Phys Rev B 76:165202
14. Janotti A, Van de Walle CG (2009) Fundamentals of zinc oxide as a semiconductor. Rep Prog Phys 72:126501
15. Kansy J (1996) Microcomputer program for analysis of positron annihilation lifetime spectra. Nucl Instrum Methods Phys Res A 374:235–244
16. Karbowski A, Fidelus JD, Karwasz GP (2011) Testing an Ortec Lifetime System. Mater Sci Forum 666:155–159
17. Katerinopoulou A, Balic-Zunic T, Lundegaard LF (2012) Application of the ellipsoid modeling of the average shape of nanosized crystallites in powder diffraction. J Appl Crystallogr 45;1:22–27
18. Li D, Leung YH, Djurisic AB *et al*. (2004) Different origins of visible luminescence in ZnO nanostructures

fabricated by the chemical and evaporation methods. Appl Phys Lett 85;9:1601–1603
19. Lin BX, Fu ZX, Jia YB (2001) Green luminescent center in undoped zinc oxide films deposited on silicon substrates. Appl Phys Lett 79:943–945
20. Liu X, Wu X, Cao H, Chang RPH (2004) Growth mechanism and properties of ZnO nanorods synthesized by plasma-enhanced chemical vapor deposition. J Appl Phys 95;6:3141–3147
21. Mishra AK, Chaudhuri SK, Mukherjee S, Priyam A, Saha A, Das D (2007) Characterization of defects in ZnO nanocrystals: Photoluminescence and positron annihilation spectroscopic studies. J Appl Phys 102:103514
22. Mo CM, Li YH, Liu YS, Zhang Y, Zhang LD (1998) Enhancement effect of photoluminescence in assemblies of nano-ZnO particles/silica aerogels. J Appl Phys 83:4389–4391
23. Qiu J, Li X, He W *et al*. (2009) The growth mechanism and optical properties of ultralong ZnO nanorod arrays with a high aspect ratio by a preheating hydrothermal method. Nanotechnology 20;15:155603
24. Ramani M, Ponnusamy S, Muthamizhchelvan C (2012) Zinc oxide nanoparticles: A study of defect level blue-green emission. Opt Mat 34:817–820
25. Shan FK, Liu GX, Lee WJ, Lee GH, Kim IS, Shin BC (2005) Aging effect and origin of deep-level emission in ZnO thin film deposited by pulsed laser deposition. Appl Phys Lett 86:221910
26. Sharma SK, Pujari PK, Sudarshan K *et al*. (2009) Positron annihilation studies in ZnO nanoparticles. Solid State Commun 149:550–554
27. Tuomisto F, Saarinen K, Look DC, Farlow GC (2005) Introduction and recovery of point defects in electron-irradiated ZnO. Phys Rev B 72:085206
28. Vanheusden K, Seager CH, Warren WL, Tallant DR, Voigt JA (1996) Mechanisms behind green photoluminescence in ZnO phosphor powders. Appl Phys Lett 68;3:403–405
29. Wang D, Chen ZQ, Wang DD *et al*. (2010) Positron annihilation study of the interfacial defects in ZnO nanocrystals: Correlation with ferromagnetism. J Appl Phys 107:023524
30. Wang D, Reynolds N (2012) Photoluminescence of zinc oxide nanowires: the effect of surface band bending. Condens Matter Phys 2012:950354
31. Wei X, Man B, Xue C, Chen C, Liu M (2006) Blue luminescent center and ultraviolet-emission dependence of ZnO films prepared by pulsed laser deposition. Jpn J Appl Phys, Part 1 45:8586–8591
32. Xiong G, Pal U, Garcia Serrano J (2007) Correlations among size, defects, and photoluminescence in ZnO nanoparticles. J Appl Phys 101;2:024317
33. Zeng H, Cai W, Hu J, Duan G, Liu P, Li Y (2006) Violet photoluminescence from shell layer of Zn/ZnO core-shell nanoparticles induced by laser ablation. Appl Phys Lett 88:171910
34. Zhao QX, Klason P, Willander M, Zhong HM, Lu W, Yang JH (2005) Deep-level emissions influenced by O and Zn implantations in ZnO. Appl Phys Lett 87;21:211912